J Therm Anal Calorim (2012) 109:153–161
DOI 10.1007/s10973-011-1575-9

Calorimetric characterization of Portland limestone cement produced by intergrinding

V. F. Rahhal · E. F. Irassar · M. A. Trezza · V. L. Bonavetti

Received: 17 February 2011 / Accepted: 7 April 2011 / Published online: 22 April 2011

Abstract The calorimetric technique provides continuous, direct, and general measurements of the course of coexisting reactions and their interactions during hydration of blended cement at early age. In this article, this technique is used to analyze the influence of compositional and process variables on the early age hydration of Portland limestone cements (PLC) made by intergrinding in a full size-cement plant. Eight cements, the vertices of 2^3 factorial design, were made with a limestone filler content (*LF*) of 0 and 24%, a gypsum content (*GC*) of 2.5, and 5.0%; and a fineness, measured as that fraction retained on a 45 μm sieve (*R45*), of 5 and 18%, to study their effects on the heat released. In addition, a PLC with a composition nearly to the center point of 2^3 designs was analyzed. Measurements were performed on cement pastes ($w/cm = 0.4$) using a semiadiabatic differential calorimeter operating at 20 °C during 48 h. At different time, the heat released was determined and it was modeled using a linear mathematical model including the three variables (*LF*, *R45*, *CG*) and their interactions. The significance of the model, the variables and the interactions was judged using the analysis of variance. Results of model show that heat released is reduced by *LF* due to physically dilution phenomenon, which is directly proportional to *LF* content. The *R45* exerts its major influence during the development of second peak (12–21 h) but later its effect declines to null contribution. *GC* retards and attenuates the hydration reactions moderately until 30 h, and then its increase contributes to Q_t due to the formation of ettringite and its transformation. The only significant interaction was *LF* with *R45* during the second peak development. Results present good correlation with the isolate measurement of compressive strength at 12, 24, and 48 h.

Keywords Portland cement · Hydration · Heat of hydration · Limestone filler · Gypsum · Fineness · Experimental design

V. F. Rahhal · E. F. Irassar (✉) · M. A. Trezza · V. L. Bonavetti
Departamento de Ingeniería Civil, Facultad de Ingeniería, Universidad Nacional del Centro de la Provincia de Buenos Aires, B7400JWI Olavarría, Argentina
e-mail: firassar@fio.unicen.edu.ar

Introduction

The cement hydration begins around the cement clinker particles interacting with dissolved ions in solution and the properties of cement paste, such as heat generation, strength development and shrinkage, are the result of the interrelated chemical, physical, and mechanical processes [1]. The course of hydration (induction, acceleration, and desacceleration) is governed by different laws: dissolution, nucleation/growth, and diffusion. It also produces the change from plastic to rigid state of paste during setting and then the reduction of porosity contributing to increase the strength and to reduce the permeability. During hydration, volume changes are also observed in paste [2].

The factors that exert major influence on the hydration kinetics of blended cement paste are: the mineralogical composition of clinker [3], the gypsum content [4], the initial water-to-cement ratio (*w/cm*) [5], the particle size distribution [6], the dispersion/flocculation state of the particles [7], the type and amount of mineral addition used [8, 9], the presence of chemical admixtures [10] and the curing temperature [11].

The production of Portland limestone cement (PLC) rises around the world due to environmental goals required

by industry. This type of cement consumes low natural raw materials, saves fuel energy for clinker production and reduces CO_2 emissions [12, 13]. For PLC produced by intergrinding, several factors can be fixed to study its influence on the hydration, but others are the consequence of the production process and they could not be controlled. For example, the particles size distribution (PSD) of intergrinding PLC depends on grinding system, mill operation, the relative gradability of component, and the amount of limestone added to cement [14, 15]. Thereafter, the size of clinker grains resulting from intergrinding process determines the kinetics of early hydration and consequently the rate of heat released, strength development and change of volume of PLC. When limestone filler is incorporated to cement, three main physical effects are observed on cement hydration [16, 17]: (a) the dilution effect, which is equivalent to an increase in the water–cement ratio, is inversely proportional to the replacement level; (b) the effect of the particle size distribution is related to limestone grains interpose between cement grains separating and dispersing the reactive grains; and (c) limestone grains act as nucleation centers for CH, accelerating the dissolution process and stimulating the hydration of cement. Depending on the amount and the fineness of limestone particles, the acceleration of the hydration can compensate the adverse effect of dilution during early age [18]. In addition, the gypsum content in cement modifies its early hydration depending on composition and PSD of clinker [4]. Gypsum participates during the dissolution and hydrolysis processes increasing the pH of the solution and finally reacts with aluminum bearing phases to form ettringite (AFt) and/or monosulfoaluminate (AFm). In PLC, the $CaCO_3$ dissolved from limestone also reacts with alumina phases to form monocarboaluminate (AFm) and it also contributes to ettringite stabilization [19]. The interaction of gypsum with limestone during early hydration of C_3A can also interfere on the setting time and the early strength depending on the cement composition and the PSD of reagents [20].

The curve of heat released is the envelope of all actions and their interactions between several factors that determines the hydration process of PLC. Calorimetric technique provides a continuous, direct and general measure of the course of coexisting process, their interactions, and the secondary effects in blended cementitious systems [21]. It is a convenient method to study the early stages of hydration because it permits to analyze simultaneously the change of cement composition, the gypsum content, the limestone content, and the particles size distribution resulting from intergrinding production of PLC.

This article describes the development of a statistical model, based on semi-adiabatic differential calorimetric measurements, which leads to the quantification of effect of fineness, gypsum, and limestone content on PLC hydration because of individual and coupled contributions at early age.

Materials and methodology

The materials selected were:

- Portland clinker from the same raw materials and industrial process with a lime saturation factor (LSF) of 0.97 ± 0.01, aluminates modulus of 1.06 ± 0.01 and silica modulus of 3.19 ± 0.02. The potential composition of the clinker calculated by Bogue was 64.6% C_3S, 16.9% C_2S, 3.9% C_3A, and 10.6% C_4AF.
- Natural gypsum stone ($CaSO_4{\cdot}2H_2O > 92\%$).
- Good quality limestone containing 88.6% $CaCO_3$ as calcite, without clay, and with quartz as the main impurity.

Table 1 reports the chemical composition of Portland clinker, limestone, and gypsum used. With these materials, eight cements were produced in industrial cement plant, where limestone filler content (*LF*), gypsum content (*GC*), and fineness (*R45*), measured as the residue on a 45 μm sieve were chosen to accomplish the experimental points of 2^3 factorial design. Experimental design consists of eight factorial points where *LF* was 0 and 24%, *GC* was 2.5 and 5.0%, and *R45* was 18 and 5%. GC and LF upper levels were selected as the maximum limit allowed by the IRAM 50000 for PLC. The low level of GC was selected as the minimum to achieve the standard setting time. R45-levels were selected to obtain a PLC with strength class of 40 or 50 (compressive strength of 40–60 MPa or >50 MPa at 28 days, respectively). In addition, a cement (P9) with a composition nearly to the experimental center point of the design (*LF* = 12%, *GC* = 3.75%, and *R45* = 12%) was included. The variables of the cements used in this experimental design in absolute and coded values are reported in Table 2.

Table 1 Chemical composition of Portland clinker, limestone, and gypsum used

Chemical composition/%			
	Clinker	Gypsum	Limestone filler
SiO_2	22.88	–	7.02
Al_2O_3	3.69	–	0.94
Fe_2O_3	3.49	–	0.40
CaO	66.55	–	51.35
MgO	0.72	–	0.34
K_2O	1.06	–	0.39
SO_3	0.90	42.90	0.03
LOI	0.71	20.50	39.5

Table 2 Composition, results of standard requirements and fineness for studied cements

Cement	Absolute value			Coded value			LOI/%	SO_3/%	Retained on sieve/%		RRSB parameters*		Blaine SS/m^2/kg	Water demand/%	Setting time/min		Compressive strength/MPa	
	LF	R45	GC	LF	R45	GC			75/μm	45/μm	x'/μm	n			Initial	Final	7 d	28 d
P1	0	5.0	2.50	−1	−1	−1	0.8	2.46	<0.1	5.2	17.9	0.93	362	28.0	140	200	44.2	55.2
P2	0	5.0	5.00	−1	−1	1	0.9	2.94	0.1	5.0	18.0	0.93	364	28.4	155	215	50.4	63.0
P3	0	18.0	2.50	−1	1	−1	0.6	2.21	4.0	17.2	24.7	0.95	261	27.0	170	240	38.3	54.7
P4	0	18.0	5.00	−1	1	1	1.0	3.27	4.8	18.0	26.5	0.94	271	27.6	180	255	37.5	50.2
P5	24.0	5.0	2.50	1	−1	−1	10.0	1.77	0.1	6.5	12.4	0.85	450	27.0	150	225	41.7	51.6
P6	24.0	5.0	5.00	1	−1	1	10.7	2.97	0.1	6.0	12.2	0.84	500	27.4	155	230	41.7	48.5
P7	24.0	18.0	2.50	1	1	−1	10.4	1.78	4.1	19.4	19.6	0.88	357	26.2	165	235	34.7	46.9
P8	24.0	18.0	5.00	1	1	1	11.1	2.78	4.5	19.7	20.5	0.85	398	26.2	190	260	33.7	43.2
P9	12.0	11.5	3.75	0	0	0	5.7	2.50	2.6	15.3	21.7	0.93	318	26.8	195	265	40.7	52.4

x' characteristic diameter and n the uniformity index of the RRSB distribution function

Cements were produced by intergrinding with two different fineness levels (18 and 5% *R45*) using an industrial ball mill with two-compartments which is integrated to a closed milling circuit equipped with a high efficiency separator. To limit the experimental program, the same dose (0.3 l/tn) of grinding aid admixture (CBA, Grace) was incorporated for all cements. In practice, portland cements are often produced without grinding aids.

Results of test for cement standard requirements are reported in Table 2. In addition, the residue on 45 μm was also determined and the PSD was measured using laser granulometer equipment (CILAS 920L). PSD results are reported in Table 2 by the uniformity index (n) and the characteristic diameter (x') of the Rosin–Rammler–Springer–Bennett (RRSB) distribution function.

The heat release was measured on cement pastes ($w/cm = 0.4$) using a semi-adiabatic differential calorimeter operating at 20 °C. Temperature was recorded during the first 48 h of hydration and the heat released was calculated as the integral below the heat dissipation rate curve versus time using a similar procedure to EN 196-9. Table 3 reports the calculated heat released (Q_t) during the first 48 h for each cement. It is reported at 3 h interval up to 30 h and subsequently at 6 h interval.

To model the influence of each selected variable on the heat released at different time (Q_t), a linear mathematical model including the three analyzed variables (*LF*, *R45*, *GC*) and their interactions was proposed as:

$$Q_t = \alpha_0 + \alpha_{LF}LF + \alpha_{R45}R45 + \alpha_{GC}GC + \alpha_{LF\times R45}LF \times R45 + \alpha_{LF\times GC}LF \times GC + \alpha_{R45\times GC}R45 \times GC + \varepsilon \quad (1)$$

where α_i are the coefficients that measure the contributions of independent variables to the heat released at given time and ε is the random error term representing the effects of uncontrolled variables. In this equation, the third order interaction term was ignored.

For the data processing and calculation of model coefficients, Design-Expert® software (Stat Ease Inc, MN,

Table 3 Calculated heat released (J g^{-1}) at different time for studied cement

Cement	Time/h												
	3	6	9	12	15	18	21	24	27	30	36	42	48
P1	16.8	37.1	72.2	103.1	124.7	140.4	152.7	163.1	171.9	179.8	192.8	203.1	211.8
P2	20.4	42.2	75.9	108.2	132.1	149.5	163.9	176.5	187.7	197.8	214.9	227.8	238.4
P3	15.8	30.5	57.4	87.5	110.4	128.2	142.3	154.1	164.3	173.4	188.6	199.6	208.0
P4	16.3	33.1	60.6	88.0	110.4	128.4	143.8	157.6	170.2	182.0	202.2	219.9	235.1
P5	10.7	24.0	43.1	65.0	86.0	103.0	116.2	126.7	135.8	143.3	156.5	167.7	178.1
P6	13.3	32.2	53.5	72.8	90.4	106.0	118.6	128.8	137.3	144.4	155.6	163.7	170.4
P7	10.3	25.1	44.0	64.1	81.8	96.2	108.3	118.6	127.2	134.5	146.0	154.9	162.4
P8	10.9	27.1	47.7	68.0	86.3	102.4	116.6	128.7	138.8	147.4	162.1	175.0	186.4
P9	14.7	31.9	56.3	81.5	105.0	123.6	138.9	152.1	163.9	174.0	191.2	205.1	216.6

USA) was used. The analysis of variance (ANOVA) was made to judge the significance of the model, the significance of each variable of the model, and the linearity of the model using the curvature test. The model is considered statistically significant when the F-test gives a probability less than 0.05. At each age, the significance of each variable was evaluated using F-value resulting form the test for comparing the variance associated with that variable with the residual variance. A variable of the model is significant (S) when the probability is less than 0.05, indicating the contribution of the proposed variable on the heat released. Significance is uncertain (US) when probability has a value between 0.05 and 0.10. Finally, the variable is non-significant (NS) when its probability has a value greater than 0.10. When ANOVA output indicates that variable was NS, it was eliminated from the model and the significance of each variable was calculated again. The curvature-test evaluates the model adequacy with respect to second-order terms, when the curvature-test is statistically significant; the calculated value of heat released for the center point composition presents a large difference with the value measured on P9 cement [22]. For validation of the model, the graphical residual analysis was used and the R^2 statistic was also calculated. Table 4 reports the significance and the curvature test for model. In this table, the coefficients of the 2^3 model are also reported: the independent coefficient (α_0) represents the heat released for the center point (cement P9) and the variable coefficient (α_i) is the variation (+ or −) into the lower and upper levels of the factor. A negative coefficient indicates that an increase of this variable result in a reduction of the heat released.

X-ray diffraction (XRD) tests were conducted on 24 and 48 h pastes prepared with the same *w/cm* ratio as used for the calorimetric samples. Pastes were hydrated at 20 °C and the hydration stopped by immersion in acetone. Then the paste was dried at 40 °C and ground to a particle size less than 45 μm. XRD measurements were performed on a diffractometer (Philips X'Pert) equipped with a graphite monochromator using CuKα radiation and operating at 40 kV and 20 mA. Step scanning was made from 5 to 35° 2θ using a scan speed of 2°/min and a sampling interval of 0.02° 2θ.

Compressive strengths was determined on mortar specimens (40 × 40 × 160 mm—Flow = 130 ± 10%) made of cement, sand, and water (1:2:0.40), which were cured in a moist cabinet at 20 ± 2 °C and removed from the moulds before testing at 12, 24, and 48 h. Reported values are the average, satisfying that the standard deviation is less than 5% of the average value.

Results and discussion

Figure 1 shows the calorimetric curves up to 48 h of eight cements of experimental design. Portland cements and PLC curves show a typical form of ΔT-time evolution. First, it shows a high rate of ΔT during the 15 min which is the results of wetting and the initial hydrolysis of C_3S and aluminates phases. It is followed by a valley corresponding to the dormant period where the concentration of species in solution increases until promoting the C_3S reaction. The second peak is the acceleration of reactions due to the

Table 4 Results of ANOVA for Q_t model indicating the significance of the model, the curvature test, values of coefficients (α_i) and significance of each term of model and the R^2 statistic

Time/h	Model		Curvature		α_i coefficients								R^2
	Prob > F	Signif*	Prob > F	Signif*	α_0	α_{LF}	Signif*	α_{R45}	Signif*	α_{GC}	Signif*	α_{LFxR45}	Signif*	
3	0.0037	S	0.7243	NS	14.3	−3.0	S	−1.0	US	0.9	US		NS	0.955
6	0.0215	S	0.8815	NS	31.4	−4.3	S	−2.4	US	2.2	US		NS	0.891
9	0.0052	S	0.8608	NS	56.8	−9.7	S	−4.4	S	2.6	US	3.1	S	0.984
12	0.0013	S	0.8016	NS	82.1	−14.6	S	−5.2	S	2.2	US	3.8	S	0.994
15	0.0010	S	0.3945	NS	102.8	−16.6	S	−5.5	S	2.0	US	3.4	S	0.995
18	0.0018	S	0.2283	NS	119.3	−17.4	S	−5.5	S	2.3	US	2.8	US	0.992
21	0.0029	S	0.1782	NS	132.8	−17.9	S	−5.0	S	2.9	US	2.6	US	0.989
24	0.0016	S	0.1974	NS	144.3	−18.6	S	−4.5	US	3.6	US		NS	0.971
27	0.0016	S	0.1394	NS	154.2	−19.4	S	−4.0	US	4.4	US		NS	0.971
30	0.0007	S	0.1629	NS	162.8	−20.4	S		NS	5.1	US		NS	0.944
36	0.0005	S	0.1046	NS	177.3	−22.3	S		NS	6.4	S		NS	0.952
42	0.0007	S	0.1008	NS	189.0	−23.7	S		NS	7.6	S		NS	0.945
48	0.0016	S	0.1345	NS	198.8	−24.5	S		NS	8.7	S		NS	0.925

* Significance: *S* Significant; *NS* no significant; *US* uncertain significance

silicate hydration with the initial precipitation of the C–S–H and CH, primarily from C_3S, and a shoulder may be observed at the descending branch of the second peaks, which is probably due to renewed ettringite (AFt) formation. A third peak due to the transformation of AFt to monosulfoaluminate (AFm) is absent or overlapping due to the low C_3A content of used cement (3.9%) [3]. Finally, hydration reactions slow gradually down and reach to very low rate after 2 days, limited by diffusion of dissolved ions through the layers of hydrates formed around the clinker grains.

For cements without limestone filler (Fig. 1a, b), finer cements as expected hydrate fast resulting in a higher initial rate of heat release at early time. But later heat released is nearly equivalent. During the first peak, the temperature of finer cement (P1 and P2) rise up to 4.7 and 3.7 °C; while it grows up to 3.5 and 3.2 °C for coarse cements (P3 and P4). The large surface area of cement exposed to water (Blaine′-specific surface increases approximately 100 m^2/kg when the *R45* changes from 18 to 5%) increases the hydrolysis. Gypsum affects the occurrence of first minimal favoring the dissolution rate (P2 < P1 and P4 < P3), causing a drop of temperature. However, the mixing procedure could influence on the ΔT measurement due to the short time to achieve the thermal equilibrium of paste mass. Therefore, the first peak could not be measured accurately.

After 2 h, the lowest point of the curve is recorded and ΔT in samples is 0.7–0.9 °C. The duration of the dormant period ($\sim$140 min) is comparable for all cements.

During the second peak, the rate of hydration is governed by the particle size of cement. When increasing the *R45*, the characteristic diameter (x') of cement increases from 18 to 25 μm. For finer cements (P1 and P2), the shape of second peak is narrow, while the acceleration rate of the hydration (slope of curve ΔT-time) is higher and its maximum value is also higher. Naturally, finer cements hydrate rapidly and release large amount of heat in short time as described experimental and numerical simulation [6]. For the studied range gypsum content does not modify the acceleration rate for the same *R45*, but it produces a wider second peak for the maximum level (*R45* = 5%) and delays the time for the maximum in coarse cements. A wider peak indicates the interaction of gypsum with the aluminates phases and/or its contribution in the C–S–H formation. Results are similar to obtained by Bentz et al. [6] for low C_3A cement and a D_{50} particle size of 5 and 30 μm using computer simulation.

Later, the descending branch of ΔT-time curve is more pronounced for finer cements (P1 and P2). Hydration of coarse cements (P3 and P4), containing more proportion of particles in large size, continues and the ΔT recorded is higher. At first time, finer cements present higher rate of heat released, but later finer and coarse cements are nearly equivalent. For the same fineness, the increase of gypsum content also produces a greater ΔT in paste.

For cement with limestone filler (Fig. 1c, d), the first peak is lower attaining to ΔT of 2.5–1.8 °C for fine (P5 and P6) and coarse (P7 and P8) cements, respectively. Instead of the lower characteristic diameter (x' = 12 and 20 μm) of PLC, less rise of temperature is expected due to the dilution effect produced by *LF*, which is relatively insoluble. Therefore, variation of temperature decays up to minimum of 0.55–0.45 °C at approximately 2 h.

After dormant period, the rate of hydration in the ascending branch is much lower than the corresponding to

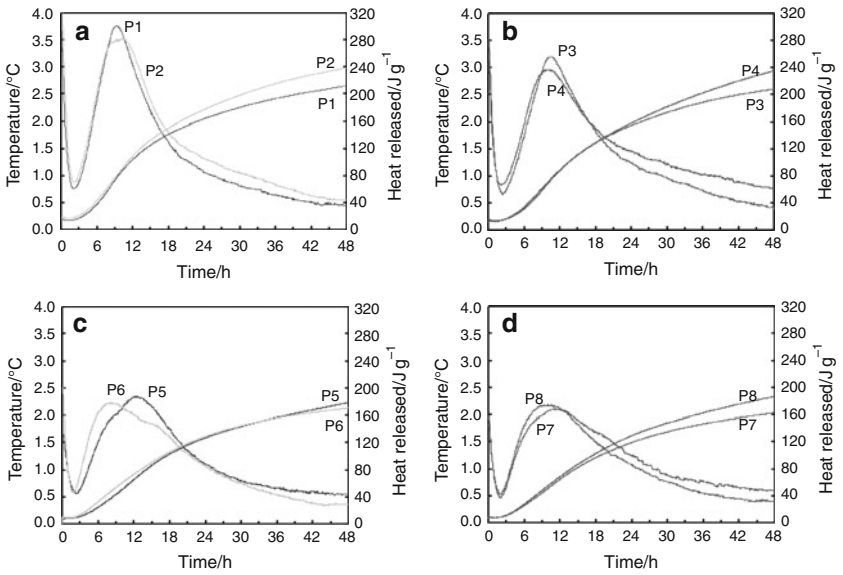

Fig. 1 Calorimetric test for **a** finer PC with 2.5 and 5% of gypsum; **b** coarse PC with 2.5 and 5% of gypsum; **c** finer PCL with 2.5 and 5% of gypsum; **d** coarse PCL with 2.5 and 5% of gypsum

cement without limestone and it decreases for coarse PLC. For PLC, the characteristic diameter is 5–6 μm smaller than the corresponding PC with the same *R45*, but some proportion is not reactive. The second peak is lower and wider due to less reactive material and the coarse size of reactive particles. Limestone filler tends to reduce both the peak rate and the amount of heat released, as reported by several authors for PLC when limestone was introduced by blending or intergrinding [23–25].

For PLC with 2.5% of gypsum (P5 and P7), the curve exhibits a noticeable shoulder after the second peak attributable to AFt formation and its transformation, as described by other authors [26]. This shoulder is smaller in PLC with 5% of gypsum (P6 and P8) and the maximum peak occurs earlier. Barker and Matthews [23] reported that the timing of the peak depends on the manufacture process of the PLC. For these cements, there is an acceleration of the maximum peak for PLC with high *GC* and some retardation for PLC with low *GC*.

Figure 2 shows the calorimetric curve for P9-cement (center point of factorial design), for comparative purposes this figure also includes the calorimetric curve for P1 and P8 cements. After mixing, the temperature rise (2.85 °C) and the drop-rate of first peak presents an intermediate value between finer PC (P1) and coarse PLC (P8). The acceleration slope and the temperature of second peak are also intermediate, but this peak is wider. Descending branch present a large ΔT that those of PC or PCL, attaining to the same value at 48 h.

Table 3 reports the calculated heat released at different time of hydration. It can be clearly observed, that *LF* reduces the heat due to physically dilution, but the influence of *R45* and gypsum depend on the time. The result of the mathematical model (Table 4) can help to analyze the influence and significance of each variable on the time.

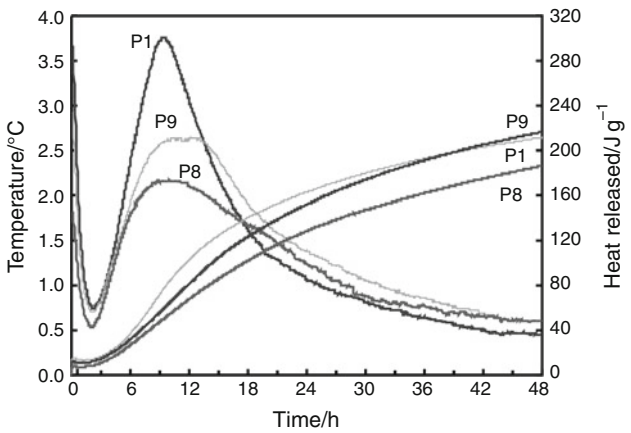

Fig. 2 Calorimetric curve for P9 cement compared with those of P1 and P8 cements

Firstly, it can be pointed about that there is a time dependence of significance of each variable:

- *LF* is a significant variable at all analyzed ages (3–48 h) and its coefficient (α_{LF}) is negative indicating that the increase of *LF* for the center point design (P9 cement) reduces the Q_t, while the reduction of *LF* increases it.
- *R45* appears as uncertain variable at 3 and 6 h, but it has an important effect on Q_t from 12–21 h. Therefore, it is again an uncertain variable at 24 and 27 h, and later it has no significant effect on the Q_t. Naturally, the negative coefficient of α_{R45} indicates that coarse cements (high *R45*) develop low Q_t at all studied ages.
- *GC* has an uncertain effect until 30 h when it varies from 2.5 to 5.0%, and then it is a significant variable contributing to Q_t when it increases.
- *LF* × *R45* interaction is significant from 9 to 15 h; it became as uncertain up to 21 h and later it was no significant variable on Q_t.

Second, it is possible to analyze the magnitude of the influence of each variable on Q_t. Figure 3 presents the influence of *LF*, *R45*, *GC* and the interaction *LF* × *R45* on the heat released at different ages. The heat variation is referenced to the composition of center point of design (P9-cement) and it was calculated as the α_i-coefficient divided the α_0-coefficient of the model. For *LF* (see Fig. 3), the decrease or increase from center point (12% *LF*) produces a significantly variation of heat released due to the dilution effect. This variation is more significantly up to 18 h, and then it is relatively constant and similar to the *LF* in cement.

From 6 to 12 h, *R45* has a large influence on heat released causing a rise of more than 10%. The development

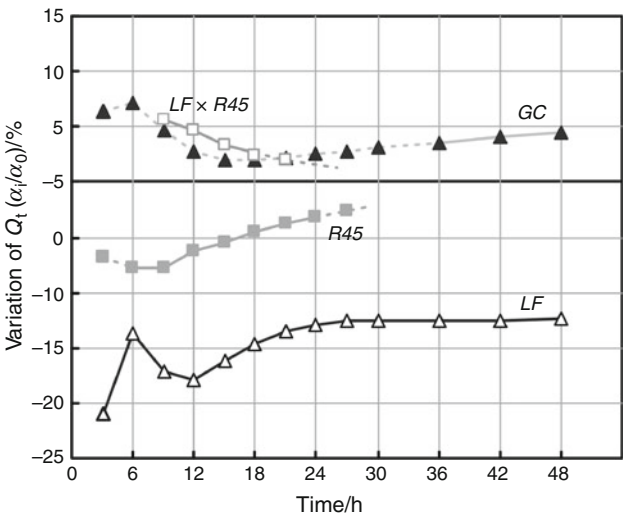

Fig. 3 Calculated effect of each variable on heat release at this time (relative value in percent)

of second peak (acceleration rate, high, and wide) is the most affected by *R45*. After 24 h, its effect declines causing a low to null variation on heat released for the analyzed system. This behavior is related to the number of particles that react simultaneously contributing to heat released. The interaction of *R45* with *LF* can also be justified because when *LF* is incorporated some finer particles are not reactive, then the model uses this term to correct the amount of reactive finer particles, and it has a positive effect.

Gypsum produces a positive contribution to the heat released during the firsts 48 h. But, its variation produces an effect of less than 5% on the total heat released until 30 h. After 36 h *GC* contributes significantly to Q_t and it can be attributable to the formation of AF phases detected by XRD analysis.

Figure 4 shows XRD-patterns for hydrated paste of coarse cements (*R45* = 18%) with different gypsum contents, either with or without limestone filler. For cement without limestone filler, the intensity of CH peaks grows significantly from 24 to 48 h and consequently C_3S peaks

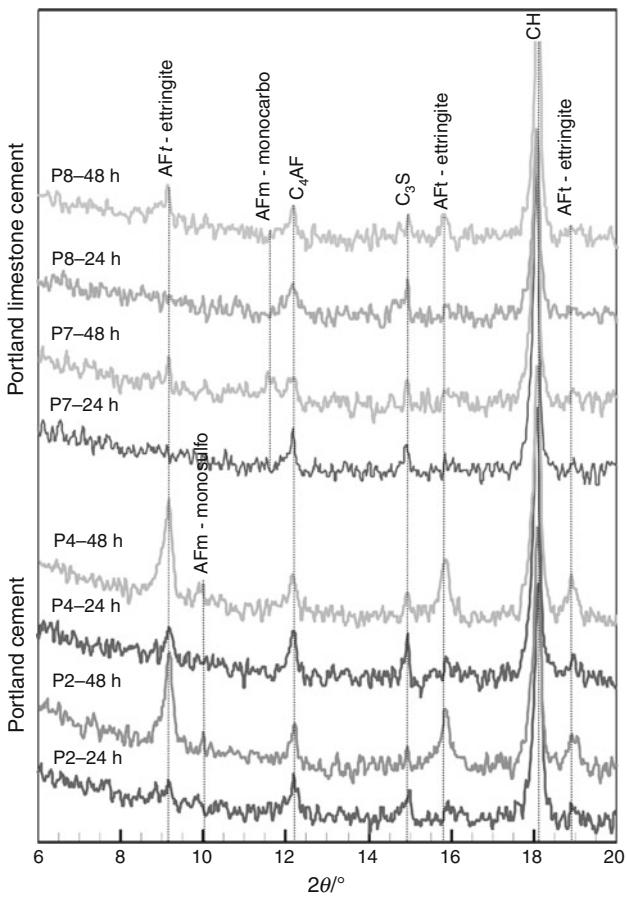

Fig. 4 XRD-patterns of hydrated paste of coarse cements (*R45* = 18%) with different gypsum contents, either with or without limestone filler at 24 and 48 h

deceases. The main difference between the P2 and P4 cements is the intensity of ettringite peaks at 24 h in cement with high *GC* (P4) and the slight peak around ($2\theta = 10.0°$) at 48 h attributable to the formation of monosulfoaluminate (AFm) in P2 cement. For cements with limestone filler, the intensity of CH and unhydrated cement peaks are less than in the corresponding P2 and P4 cements due to dilution effect. The main difference is the low intensity of ettringite peaks, absent at 24 h, and the presence of monocarboluminate in the P7 cement after 48 h due to its high stability, compared to monosulfoaluminate [19]. The low intensity of ettringite peaks can also be attributable to dilution, but its presence and the occurrence of the AFm phase corroborates the significance of *GC* in the model of heat released at later ages. For the cement composition, ettringite from C_4AF also contributes to the calorific synergy effect [27].

In order to validate the influence of these variables on the kinetics of hydration of integrinding PLC, subsequently the obtained results are compared with the compressive strength of mortar. The expression that correlates the compressive strength and the progress of hydration of cement is the gel/space ratio (X) proposed by Powers [28]. X is defined as the ratio of the volume of the volume of hydration products (V_g) to the sum of the volumes of the hydrated cement and capillary pores. According to Powers′ model applied to PLC [29, 30], the volume of hydration products (V_g) is proportional to the degree of hydration of cement (α) and the filler content (V_f) in the cement. Then, this expression becomes as $0.694\ \alpha\ (1-V_f)$, which takes into account the acceleration of hydration and the dilution effect caused by limestone filler. Furthermore, dilution also affects the denominator included in the gel-space ratio, because it increase the *w/cm* ratio inversely proportionally to *LF*; then its expression is $0.319\ \alpha + (w/cm)/(1-V_f)$. The degree of hydration (α) was calculated as the ratio of heat evolved (Q_t) at 12, 24, and 48 h (Table 3) to the total (and theoretical) heat of hydration of the Portland cement Q_∞ (468 J/g for the cement used) reduced proportionally by limestone content.

Figure 5 shows the experimental values of compressive strength versus the gel/space ratio calculated. There is a good correlation between experimental and calculated values as reported previously [17, 29, 30]. In recent paper [31], it was proved that the influence of studied variables on early compressive strength is time dependent. *LF* produces a significant variation at 12 h and then it is reduced around ±10% at 48 h. *R45* variable has a large influence on very early strength producing an increase of more than 20% at 12 h and then it declines. *GC* does not cause significant changes in compressive strength at 12 h, its variation exerts a slight influence at 24 h and then it is significant at 48 h.

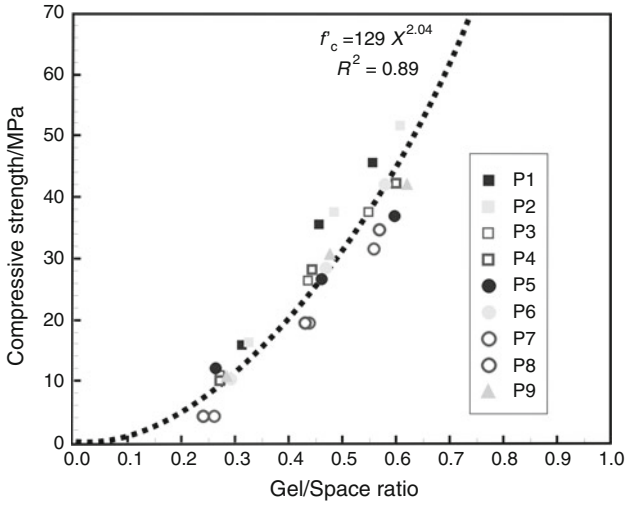

Fig. 5 Experimental values of compressive strength versus the gel/space ratio, calculated from the measured degrees of hydration 12, 24, and 48 h

Results observed for compressive strength shows the same trend as previously described in the evolution of heat released, with the advantage that this property allows continuous measurement of the influence of each variable on the hydration of cement with different fineness, limestone filler, and gypsum content.

Conclusions

Based on this experimental design made at industrial scale, the following conclusions can be drawn with respect to the effects of the limestone content, the fineness, and the gypsum content on the early hydration of PLC produced by intergrinding process:

Limestone filler is a significant variable on heat released (Q_t) during all time test (48 h). It reduces the heat due to dilution effect, which is directly proportional to *LF* content. The height of the main peak and the total heat released are modified for blended cement with the same *R45* grinding objective.

The fineness, measured as retained on sieve 45 μm, appears as significant factor on Q_t from 12 to 21 h; which is the time corresponding to the development of second peak (acceleration rate, high, and wide). Later, its effect declines causing very low variation. Coarser cements result in a lower initial heat released rate, which could be useful when thermal cracking is a concern. This behavior is related to the amount of particles that hydrates simultaneously.

The interaction of *R45* with *LF* is more significant during the development of the second peak, because the effect on heat of hydration produced by finer particles depends on the proportion of *LF* (not reactive) in this particle size of the blend. Finally, PLC could be finer but it could have a low heat released depending on *LF* content.

From 2.5 to 5.0% of gypsum added, it retards and attenuates the hydration reactions. But statistically, it has an uncertain effect until 30 h. Then, it is a significant variable contributing to Q_t when it increases because the formation of ettringite and its transformation is governed by *GC*.

From this study, the power of using a combination of calorimetric technique and the statistical experimental design to modeling continuously influence of several factors on the early hydration of blending cements produced by intergrinding has been demonstrated. This combination is correlated with isolated values of the compressive strength.

Acknowledgements This article is the result of collaboration between Cementos Avellaneda SA (Argentine) and the National University of Center of Province of Buenos Aires. Authors would also like to gratefully acknowledge Eng. Daniel Violini and Eng. Carlos Milanesi for their support during industrial process to make this research.

References

1. Bentz DP. Cement hydration: building bridges and dams at the microstructure level. Mater Struct. 2007;40(4):397–404.
2. Lura P, Winnefeld F, Klemm S. Simultaneous measurements of heat of hydration and chemical shrinkage on hardening cement pastes. J Therm Anal Calorim. 2010;101(3):925–32.
3. Odler I. Hydration, setting and hardening of Portland cement. In: Hewlett P, editor. Lea's Chemistry of cement and concrete. Butterworth-Heinemann: Elsevier; 1998. p. 241–98.
4. Frigione G. Gypsum in cement. In: Ghosh SN, editor. Advances in cement technology: chemistry, manufacture and testing. New Delhi: Tech book International; 2002. p. 87–170.
5. Bentz DP. Influence of water-to-cement ratio on hydration kinetics: simple models based on spatial considerations. Cem Concr Res. 2006;36(2):238–44.
6. Bentz DP, Garboczi EJ, Haecker CJ, Jensen OM. Effects of cement particle size distribution on performance properties of cement-based materials. Cement Concrete Res. 1999;29(10):1663–71.
7. Knudsen T. The dispersion model for hydration of Portland cement 1. General concepts. Cement Concrete Res. 1984;14(5):622–30.
8. Sharma RL, Pandey SP. Influence of mineral additives on the hydration characteristics of ordinary Portland cement. Cement Concrete Res. 1999;29(9):1525–9.
9. Talero R, Rahhal VF. Calorimetric comparison of Portland cements containing silica fume and metakaolin. Is silica fume, like metakaolin, characterized by pozzolanic activity that is more specific than generic? J Therm Anal Calorim. 2007;96(2):383–93.
10. Uchikawa H, Hanehara S, Shirasaka T, Sawaki D. Effect of admixture on hydration of cement, adsorptive behavior of admixture and fluidity and setting of fresh cement paste. Cement and Concrete Res. 1992;22(6):1115–29.
11. Escalante-Garcia JI. Nonevaporable water from neat OPC and replacement materials in composite cements hydrated at different temperatures. Cement and Concrete Res. 2003;33(11):1883–8.
12. Baron J, Dourve C. Technical and economical aspects of the use of limestone filler additions in cement. World Cement. 1987;18(4):100–4.

13. Damtoft JS, Lukasik J, Herfort D, Sorrentino D, Gartner EM. Sustainable development and climate change initiatives. Cement Concrete Res. 2008;38(2):115–27.
14. Ellerbrock HG, Spung S, Kuhlmann K. Particle size distribution and properties of cement. Part III: influence of grinding process. Zement-Kalk-Gips. 1990;43(1):13–9.
15. Tsivilis S, Chaniotakis E, Kakali G, Batis G. An analysis of the properties of Portland limestone cements and concrete. Cem Concr Compos. 2002;24(3–4):371–8.
16. Lawrence P, Cyr M, Ringot E. Mineral admixtures in mortars: effect of inert materials on short-term hydration. Cement Concrete Res. 2003;33(12):1939–47.
17. Cyr M, Lawrence P, Ringot E. Mineral admixtures in mortars: quantification of the physical effects of inert materials on short-term hydration. Cement Concrete Res. 2005;35(4):719–30.
18. Tsivilis S, Kakali G, Chaniotakis E, Souvaridou A. A study on the hydration of Portland limestone cement by means of TG. J Therm Anal Calorim. 1998;52(3):863–70.
19. Bonavetti VL, Rahhal VF, Irassar EF. Studies on the carboaluminate formation in limestone filler-blended cements. Cement Concrete Res. 2001;31(6):853–9.
20. Bensted J. Some hydration investigations involving Portland cement—effect of calcium carbonate substitution of gypsum. World Cement Technol. 1980;11(8):395–406.
21. Roszczynialski W, Nocuń-Wczelik W. Studies of cementitious systems with new generation by-products from fluidised bed combustion. J Therm Anal Calorim. 2004;77(1):151–8.
22. Montgomery DC, Runger GC, Hubele NF. Engineering statistics. New York: John Wiley; 2006.
23. Barker AP, Matthews JD. Heat release characteristics of limestone-filled cements. Performance of limestone-filled cements: report of joint BRE/BCA/Cement industry working party, 28 November 1989, Watford: Building Research Establishment; 1993.
24. Rahhal V, Talero R. Early hydration of Portland cement with crystalline mineral additions. Cement Concrete Res. 2005;35(7):1285–91.
25. Poppe AM, DeSchutter G. Analytical hydration model for filler rich self-compacting concrete. J Adv Concr Technol. 2006;4(3):259–66.
26. Xiong X, van Breugel K. Hydration processes of cement blended with limestone powder: experimental study and numerical simulation. In: Grieve G, Owens G editors. Proceedings of the 11th international congress on the chemistry of cement (ICCC) CD-ROM, Durban, 2003. p. 1983–1993.
27. Rahhal VF, Cabrera O, Delgado A, Pedrajas C, Talero R. C_4AF ettringite and calorific synergic effect contribution. J Therm Anal Calorim. 2010;100(1):57–63.
28. Powers TC. Structure and physical properties of hardened Portland cement paste. J Am Ceramic Soc. 1958;41(1):1–6.
29. Bonavetti V, Donza H, Menendez G, Cabrera O, Irassar EF. Limestone filler cement in low w/c concrete: a rational use of energy. Cement Concrete Res. 2003;33(6):865–71.
30. Bentz DP, Irassar EF, Bucher BE, Weiss WJ. Limestone fillers conserve cement-Part 1: an analysis based on Powers' model. Concrete International. 2009;31(11):41–6.
31. Irassar EF, Violni D, Rahhal VF, Milanesi C, Trezza MA, Bonavetti VL. Influence of limestone content, gypsum content and fineness on early age properties of Portland limestone cement produced by intergrinding. Cement Concrete Composite. 2011;33(2):192–200.